A Framework for Balancing Flood Control and Demand for Irrigation in Multipurpose Reservoir Management

A Thesis

Presented in Partial Fulfillment of the Requirement for the

Degree of Master of Science

with a

Major in Applied Economics

in the

College of Graduate Studies

University of Idaho

by

Tayebeh Soltaninejad

July 2015

Major Professor: Levan Elbakidze, Ph.D.

Committee Members: R. Garth Taylor, Ph.D.; Lyudmyla Barannyk, Ph.D.

Department Administrator: Christopher McIntosh, Ph.D.

Authorization to Submit Thesis

This thesis of Tayebeh Soltaninejad, submitted for the degree of Master of Science with a major in Applied Economics and titled "A Framework for Balancing Flood Control and Demand for Irrigation in Multipurpose Reservoir Management" has been reviewed in final form. Permission, as indicated by the signatures and dates given below, is now granted to submit final copies to the college of Graduate Studies for approval.

Major Professor:	______________________ Levan Elbakidze, Ph.D.	Date:	__________
Committee Members:	______________________ R. Garth Taylor, Ph.D.	Date:	__________
	______________________ Lyudmyla Barannyk, Ph.D.	Date:	__________
Department Administrator:	______________________ Christopher McIntosh, Ph.D.	Date:	__________

Abstract

Efficient water release in multipurpose reservoirs is of the utmost concern for water resource management agencies. A unique approach is presented in this study based on a dynamic optimization system to derive the optimal amount of water release during a water year that takes into consideration both irrigation demand and flood safety. The dynamic optimization model seeks to maximize benefits from water release including agricultural irrigation benefit minus flood damage. A partial differential equation resulting from the Hamilton-Jacobi-Bellman equation is solved and optimum water release is derived. The empirical model is then developed using the Lucky Peak Dam in Idaho as a case study. A nonlinear GAMS model is developed to demonstrate preliminary results for optimum water release and reservoir water levels during a water year. The empirical results are compared qualitatively to engineering operating rule curves used in reservoir operation. Implications of potential earlier run-off due to climatic change are also examined.

Acknowledgments

Foremost, I would like to express my deepest thanks to my advisor, Dr. Levan Elbakidze. His patience and encouragement were key motivations throughout my Master's. I would also like to thank Dr. Taylor and Dr. Barannyk for offering thorough and excellent feedback on my research. I am also grateful to my colleagues, Mahalingam Dhamodharan and Juan Luo for their help and time.

Most of all, I would like to thank my parents and my husband who encourage and support me.

Table of Contents

List of Figures

Chapter 1: Introduction

While dams are generally meant to provide water for agriculture and human consumption, they can also be used for other purposes such as flood control, hydropower generation, industrial applications, and recreational uses. More than 10% of American cropland is irrigated using water stored in dams (Federal Emergency Management Agency, 2014). Water release throughout the year is determined by dam operators who regulate water release based on many considerations, including amount of water in the dam, dam water holding capacity, time, irrigation demand, potential flood damages, and runoff forecast. Changes in precipitation and inflow patterns can complicate water management systems due to a shorter time frame of annual runoff or more frequent extreme weather events such as droughts and floods (Trenberth, 2011). Changes in streamflow timing can reduce water availability for irrigation, aquatic habitat, energy generation and other uses during critical seasons. On the other hand, increase in the frequency and intensity of rainfall and runoff events can lead to overloaded reservoirs and flooding (Trenberth, 2011)

What makes operating multi-objective reservoirs complex is that the individual objectives may be conflicting. Flood control requires lower water levels in the reservoir to minimize flood chances. This entails large early spring water release to make space available for potential future runoff. Meanwhile, the irrigation water needs to be stored in a reservoir to meet the high demand for irrigation water in the summer. This trade-off implies that water release should be optimized to assure availability of irrigation water during dry seasons while not exposing downstream communities to significant flood risk. Since peak irrigation demands in many cases do not coincide with the timing of water release for flood safety, the operating policies must address trade-offs between management of reservoirs for flood protection versus management for dry-season irrigation water supplies.

Reservoir operating rules are designed to control the amount of available space in the reservoir via water release to assure flood control. Schmidt et al. (2013) showed the rule curves for the Boise Reservoir system to get an idea of how flood control reservoirs are managed. Ahmad and Simonovic (2000) used system dynamic optimization model to develop operating rule curves to minimize flooding. Chen et al. (2007) developed a multi-objective genetic algorithm for optimizing the rule curves in a multipurpose reservoir in Taiwan.

Reservoir operating rules are designed to manage and operate the reservoir systems so that water release satisfies the system objectives, consistent with inflow and storage capacity. To do so, many optimization methods have been developed. For example, Chatterjee et al. (1998) proposed a dynamic model to study reservoir water allocation for hydropower generation and irrigation. They explore the time lag between peak irrigation demand and peak hydropower demand. In this context, release of irrigation water in the spring reduces the amount of water availability for hydropower production during the peak energy demand in the summer. Using a nonlinear optimization model developed for the Stanislaus and Merced irrigation district in California, Chatterjee et al. demonstrated a modified reservoir management relative to the observed releases. The modified release path was derived by solving the control models for the profit maximizing path which released less water on average during the spring and early summer months than actually occurred.

Another method for modeling reservoir operations is the system dynamics (SD) approach. SD is a feedback-based object-oriented simulation affected by its own past actions. For example, SD can be used as a tool to quantitatively simulate the process within a water resources system and use this simulation to predict the reservoir future behavior based on the historical major floods. With SD we can show how the various changes of primary elements can affect the dynamics of the system in the future. Ahmad et al. (2000) used the SD approach to model the interactive components of water cycle in reservoirs to develop reservoir operation rules for flood mitigation. They used SD to simulate the behavior of reservoir and upstream and downstream area under major past floods. Although their predictive simulation model was for a single-objective reservoir management of flood safety program, they applied this method in the single multipurpose Shellmouth reservoir on the Assiniboine River in Canada and developed operating rules for high flow years to minimize flooding. They explored five alternative operating rules by changing reservoir storage allocation and reservoir outflow. The revised operating rules produced only minor flooding risks in four out of five major flood events and exhibited an improvement of flood management capability in the Assiniboine River relative to current capacity.

Roseta-Palma and Xepapadeas (2004) examined robust control as a framework for reservoir water management decisions to explore the implications of uncertainty aversion for water release. Robust control is an optimization model, which is employed to optimize relative to worst-case scenario. Precipitation was considered as "uncertainty," which is an event whose space state of outcome is known but decision makers are unable to assign probabilities and used the uncertainty implication for quantitative water used in a static and dynamic setting. They assumed that water flow followed a stochastic process. The probability distributions were designed for each stochastic variable and for various levels of uncertainty associated with inflow. They analyzed the precautionary behavior appearing from a robust control approach for modeling water resource. They identified the possibilities of robust control approach and its connection with uncertainty aversion and precautionary behavior and compared the robust choices with those of a benchmark stochastic model. A precautionary behavior appeared in the dynamic setting where the reservoir management decision makers reduced reservoir water because of the integration of worst case precipitation.

Tresos and Yeh (1987) examined a stochastic optimization model which is applicable to constrained stochastic system with quadratic objective function and applied their model on Mammoth reservoir in California in order to explore the potential for increasing hydropower production. This study used probabilistic inflow forecasts in the decision making process. Tresos and Yeh developed an optimization model that takes into account the uncertainty of forecasting at the time of policy making. This optimization model is applicable to a system of reservoirs with can be configured as an analytical tool in the reservoir operation with high level of precipitation uncertainty.

The objective of this thesis is to propose a framework for modeling optimal reservoir water release throughout one year in order to satisfy two objectives: to balance irrigation water demand and flood control. There is a trade-off between maintaining a full reservoir for irrigation purposes and maintaining sufficient space in the reservoir to reduce flood risk. None of the previous studies have considered that economic trade-offs that involve balancing benefits and costs associated with the two objectives simultaneously. A dynamic optimization model is developed and applied to illustrate a method for analyzing the tradeoff in the optimal water release timing, taking into account the value of water release for both irrigation and flood control. The obtained optimal path of water release is qualitatively compared to the dynamic reservoir space requirement implied by the present flood control rule curves. A hypothetical irrigation water demand function, corresponding to the demand for irrigation water for growing low value crops in the Lower Boise basin irrigation water area, is used to represent the demand for irrigation water on the agricultural production side. Flood damages were obtained from the Schmidt et al. (2013) study as a function of discharge at the Glenwood Bridge gaging station for both Canyon and Ada Counties.

We used the well-established optimal control methodology (Kamien and Schwartz, 1991) for the analytical framework. Dynamic optimization is used to formulate the model, which considers both irrigation water demand and flood safety to derive optimal path for water release. This project provides a starting point for expanding the scope of the analysis in future studies. Specifically, future studies can rely on the framework in this study to examine the effect of non-stationarity runoff (Milly, 2008) on optimal reservoir management for flood control and irrigation demand. This framework can also be expanded to include other uses of the reservoir such as hydropower and in-stream flow for aquatic habitat. Such extensions will account for the effect of non-stationarity on flood frequency estimation (Raff, Pruitt and Brekke, 2009). One can expand the model to a multiyear context to allow for potential adjustments in planted crop acreages in response to possible changes in water availability across water years and irrigation seasons. Irrigation water availability can change due to potential adjustments in regulated reservoir outflows needed to balance flood control and other water uses. Multiyear stochastic modeling of optimal reservoir operations will incorporate greater inflow variability as a result of climate change with increased probability of both increased frequencies and intensities of snowmelt/runoff/ precipitation and drought conditions.

This thesis is organized as follows: In Chapter 2, I provide a theoretical illustration of the framework and present an analytical characterization of optimal intra-seasonal water release dynamics. Chapter 3 introduces a preliminary empirical application in the context of Lucky Peak Dam in the state of Idaho. Results are presented in Chapter 4. The study concludes with a discussion of results in Chapter 5.

Chapter 2: Theoretical Framework

This section provides a theoretical framework for optimal dynamic management of a water reservoir for flood control and irrigation water provision. Gross benefit of irrigation water, π, is the area under the inverse derived demand for irrigation water (Roumasset and Wada, 2013).

$$\pi = \int_0^{q(t)} D^{-1}\,(q(t), t)\; dq(t). \quad (1)$$

The flood damage function is $\Phi(q(t))$, where $q(t)$ is the amount of water released from the reservoir, and t is time from 0 to T for one water year. The objective is to optimize the water release in order to maximize benefits from irrigation water and minimize damages from floods. Hence, the objective function is agricultural benefits minus flood damages during a water year:

$$Max_{q(t)} \int_0^T \left\{ \int_0^{q(t)} D^{-1}(q(t), t)\; dq(t) - \Phi\,(q(t)) \right\} dt \;(2)$$

which is subject to the dynamics of the amount of water in the reservoir,

$$\frac{ds(t)}{dt} = \mu(t) - q(t), \;(3)$$

$$0 < s(t) \le s_{Max}, \qquad (4)$$

$$s(0) = 0. \qquad (5)$$

where $s(t)$ denotes water volume in the reservoir at t, and s_{max} denotes the capacity of the reservoir. The amount of water in the reservoir is the state variable in this dynamic optimization problem. Eq. 3 shows how the change in the water volume in the reservoir depends on inflow rate (μ) and water release rate (q).

The optimal solution for the value function is derived from the Hamilton-Jacobi-Bellman equation (Kamian and Schwartz, 1991),

$$-J_t(t, s) = Max_{q(t)}\left[f(t, s, q) + J_s(t, s)\big(\mu(t) - q(t)\big) + \theta_1(s_{Max} - \mathrm{s}) + \theta_2 s\right], \quad (6)$$

Where $f(t, s, q) = \int_0^{q(t)} D^{-1}(q(t), t)\, dq(t) - \Phi\,(\mathrm{q(t)})$, θ_1 is a dynamic Lagrange multiplier for the upper bound of the state variable, and $\theta_2$is the dynamic Lagrange multiplier for the lower bound of the state variable.

A simple linear form of an inverse derived demand for irrigation water is used (Eq. 7) which shows decreasing marginal value of irrigation water.

$$D^{-1}(q(t), t) = -aq(t) + b(t) \qquad (7)$$

b is an intercept which shifts the demand curve up and down depending on the season (i.e. irrigation, water demand increases during a dry irrigation season).

According to Schmidt et al. (2013), flood damage is an increasing function of water release volume. To obtain a tractable mathematical illustration, the flood damage function is formulated as a quadratic function:

$$\Phi(q(t)) = kq^2 \qquad (8)$$

where k is a small positive coefficient such that small values of q produce negligible values for $\Phi\,\big(q(t)\big)$ until q approaches a water release amount corresponding to a canal carrying capacity, and q $\geq$0.

Given the functional forms for irrigation demand and flood damage costs, the optimal control problem is:

$$Max_{q(t)} \int_0^T \left\{\int_0^{q(t)} (-aq + b)\, dq(t) - \mathrm{k}\, q(t)^2\right\} dt. \ (9)$$

Substituting the optimal control statement in the Hamilton-Jacobi Bellman equation, results in:

$$-J_t = Max_{q(t)}[\int_0^{q(t)} (-aq(t) + b) dq(t) - \mathrm{k}\, q(t)^{2\}}] + J_s(t, s)\big(\mu(t) - q(t)\big) + \theta_1(s_{Max} - \mathrm{s}) + \theta_2 s]. \qquad (10)$$

Suppressing t in $q(t)$, $b(t)$ and $\mu(t)$ for the sake of convenience, but keeping in mind that these parameters are functions of time, and differentiating the right hand side of Eq. 10 to find the optimal q, we get:

$$-aq + b - 2kq - j_s = 0. \qquad (11)$$

so

$$q = {}^{(-j_s + b)}\!\big/_{a + 2k}. \qquad (12)$$

The area under water demand curve is derived as:

$$\int_0^{q(t)} (-aq + b)dq(t) = \frac{-aq^2}{2} + bq + c. \qquad (13)$$

Plugging Eq. 12 and 13 into 10, we obtain

$$-j_t = \frac{-a}{2}\left(\frac{-J_s + b}{a + 2k}\right)^2 + b\left(\frac{-J_s + b}{a + 2k}\right) + c - k\left(\frac{-J_s + b}{a + 2k}\right)^2 + J_s\left(\mu - \left(\frac{-J_s + b}{a + 2k}\right)\right) + \theta_1(s_{Max} - \mathrm{s}) + \theta_2\, s. \quad (14)$$

Eq. 14 is a partial differential equation which consists of coefficient *a* and intercept *b* in the irrigation water demand function, dynamic Lagrange multipliers (i.e. θ_1 and θ_2), water volume in the reservoir, reservoir capacity, water inflow rate, and flood damage function coefficient *k*. The solution for this partial differential equation is provided in Eq. 15. The proof of solution is provided in the appendix A.

$$j(t,s) = \left(\frac{1}{2}\right)\Big(2bs - 2a\mu s - 4k\mu s + \frac{1}{12(a + 2k)(\theta_1 - \theta_2)}((2b - 2(a + 2k)\mu)^2 - 4(b^2 - C_1 + 4ck - 4k\theta_1 s + 4k\theta_2 s + 4k\theta_1 s_{max} + 2a(c - \theta_1 s + \theta_2 s + \theta_1 s_{max})))^{3/2}\Big)$$

$$-\frac{C_1 t}{2(a+2K)} + C_2 \qquad (15)$$

Taking derivatives with respect to *s* and *t*, we have

$$j_s = \frac{1}{2}\,(2b - 2a\mu - 4k\mu + \left(\begin{matrix}(2b-2(a+2k)\mu)^2 - 4(b^2 - C_1 + 4ck - 4k\theta_1 s + 4k\theta_2 s + 4k\theta_1 s_{max} + \\ 2a(c - \theta_1 s + \theta_2 s + \theta_2 s + \theta_1 s_{max}))\end{matrix}\right)^{1/2}),$$

(16)

and

$$j_t = \frac{-c_1}{2(a+2k)}. \quad (17)$$

Substituting j_s in Eq. 12 gives

$$q(t) = \frac{1}{a+2k}(b + \frac{1}{2}(-2b + 2a\mu + 4k\mu - \left(\begin{matrix}(2b-2(a+2k)\mu)^2 - 4(b^2 - C_1 + 4ck - 4k\theta_1 s + 4k\theta_2 s + 4k\theta_1 s_{max} + \\ 2a(c - \theta_1 s + \theta_2 s + \theta_2 s + \theta_1 s_{max}))\end{matrix}\right)^{1/2}).$$

(18)

Eq. 18 is then simplified as

$$q\,(t) = \mu(t) - \frac{\left(c_1 + (a+2k)\left(-2b(t)\mu(t) + (a+2k)\mu(t)^2 - 2\left(c + \theta_1 s_{max} + (-\theta_1+\theta_2)s(t)\right)\right)\right)^{1/2}}{a+2k}.$$

(19)

The value of q at the optimum includes other principal parameters and functions. By having empirical functions for $\mu(t)$ and $b(t)$, we can illustrate the behavior of these two functions over the time as shown in Chapter 3.

To show the effect of k on $q(t)$, we take the derivative of $q(t)$ with respect to *k*.

$$q_k = \frac{2\left(-C_1 + (a+2k)(c + b\mu - \theta_1 s + \theta_2 s + \theta_1 s_{max})\right)}{(a+2k)^2\sqrt{c1 + (a+2k)(-2c - 2b\mu + (a+2k)\mu^2 + 2\theta_1 s - 2\theta_2 s - 2\theta_1 s_{max})}}$$

(20)

Thus, Eq. 20 suggests that increase in flood damages (k) does not have a unidirectional effect on release. Because, the effect depends on the combination of the values of parameters for inflow, flood damage, as well as irrigation demand. On the one hand, increase in flood damages can imply more preventative release at the expense of availability of water for irrigation. On the other hand, if current release is already high then increasing release can imply significant flood damage. Because the flood damage has been defined as a function of water release. In such case, greater flood damage parameter (k) can result in reduced optimal discharge.

In general, if we could predict the inflow rate during a year and we know the water demand and flood damage functions, we can substitute all these functions in the model, which will suggest an optimal water release and reservoir water level throughout the year.

Chapter 3: Case Study

The empirical work in this study applies the above framework to the operation of the Lucky Peak Dam, which is located on the Boise River in Ada County, ID, 17 miles northeast of Boise on Highway 21 and downstream of the Arrowrock Dam. The average elevation of the full reservoir is 3,055 feet (931 m) and the drainage area is 6940 km^2 (2680 mi^2) (Raff et al., 2009). The total capacity of the reservoir is 307,000 acre-feet and the surface area is 2820 acres (BOR, 2014).

The empirical model requires information on inflows into the reservoir during a water year. We use the daily water inflow data provided by the Lucky Peak Dam operators (BOR, 2014). In addition, we need agricultural water demand and potential flood damage estimates to specify the objective function empirically. We will explain the methods to obtain these functions in sections 3.1-3.3.

3.1 Irrigation Water Demand

Agricultural water demand and flood damage functions were estimated in for the Boise Basin (Schmidt et al. 2013). Aggregate water demand for a mix of crops was calculated by horizontally adding the demand of individual crops at every price (Schmidt et al., 2013). The crops are considered as high value (cash) or low value (field) crops. The high value crops included sugar beets, herbs, dry beans, spring wheat, and potatoes, while the low value crops were alfalfa, silage corn, winter wheat, peas, and hay. The horizontal summation of crop demands is a series of points in which different croplands may drop in or out of production as the irrigation water price is changed. For instance, there may be lower production or even no production for the lower value crops when the water price is high.

Irrigation water demand in lower Boise Basin was obtained from Schmidt et al. (2013). Schmidt et al. (2013) used commodity prices and the evapotranspiration (ET) production function of Martin and Supalla (1989) to derive a static short-term irrigation water demand (Figure 0-1) following methodology described in Contor et al. (2010). This production function can be converted to an irrigation water demand by using exponents, which are related to crop irrigation efficiency. These exponents are obtained from basin-specific function and agronomic data including commodity price per yield unit, yield at full irrigation, ET depth at full yield, dry land (non-irrigated) yield, and irrigation depth at full yield. This calculator also assumed that market mechanisms have already optimized crop acreages and mix of crops, and considered the water demand as full-season volume delivered (Martin and Supalla, 1989).

In this model, the water demand for only the low value crops is included for illustration purposes. It would be straightforward to include total demand for irrigation water for all crops in the region. For illustrative purposes, the application is also limited to only the Lucky Peak Dam, which is one of six dams that provide flood control and irrigation water in the watershed. The water demand curve for low value (field) crops is shown in Figure 0-1.

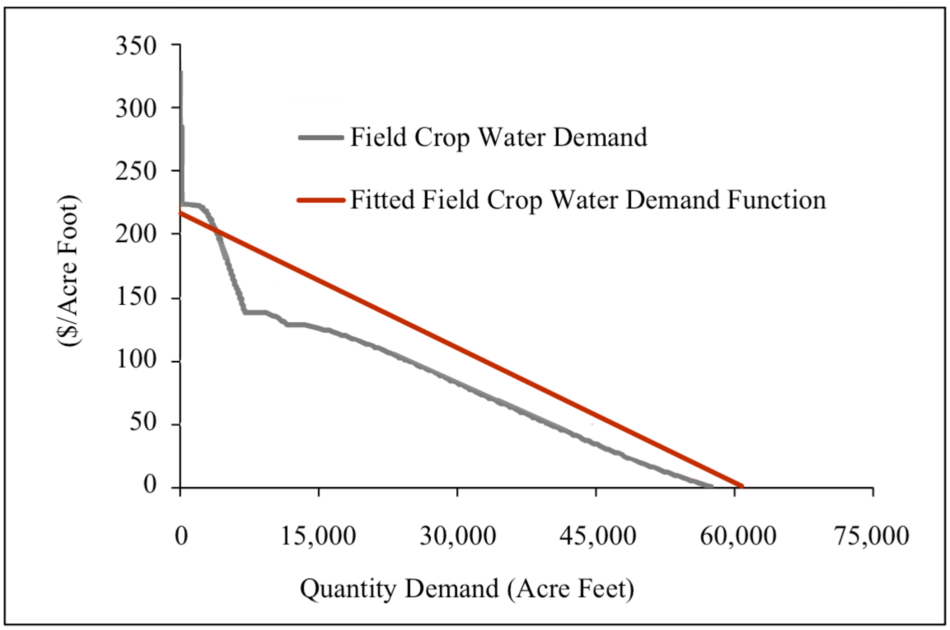

Figure 0-1 Irrigation water demand for low value (field) crops (Schmidt et al., 2013). The function is fitted linearly as $P = -0.0036\ q + 220$.

For simplicity, the agricultural water demand is assumed to be a linear function(Figure 0-1). The water demand intercept, *b*, and the water demand slope, *a*, of the linear function are calculated as *a*= 0.0036 and *b*= 220, respectively.

Irrigation water demand shown in7 is a function of time. It is assumed that the linear water demand function is varying in slope (*a*) and y-intercept (time dependent *b*) throughout the year. The irrigation water demand in Eq. 7, (Figure 3-1) does not consider the time dependency or seasonal demand of irrigation water demand. In order to make the demand function flexible to change through seasons and show how the demand function behaves empirically, a GAMS program was developed to express the irrigation water demand scale parameter varying throughout the water year (shown in Figure 0-2)

Water demand (Figure 3-1), the scale parameter, ψ, is multiplied by b and a and expressed as

$$\psi(t) = -1\times10^{-6}t^2 + 6\times10^{-4}t - 0.0667, \quad (21)$$

Indeed, including ψ in the water demand equation let us show the seasonality of agriculture water demand. The ψ calculation is explained in appendix C.

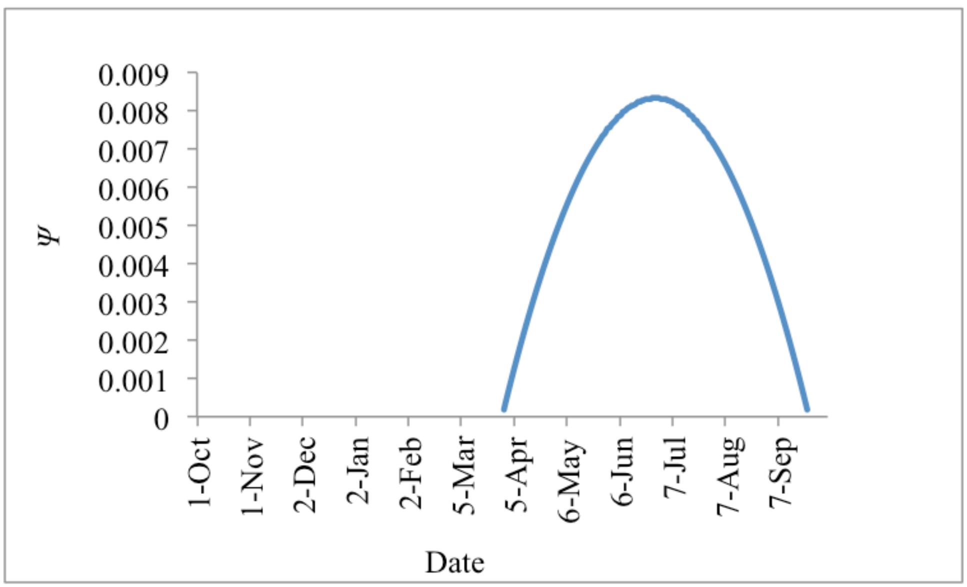

Figure 0-2 Irrigation water demand timing during a water year.

3.2 Flood Damage

The flood damage cost function was retrieved from the study by Schmidt et al. (2013). The target location for the Boise River flood flow calculation in this study is Glenwood Bridge gaging station. They used a frequency curve averaging technique to approximate the recurrence of unregulated flows. The maximum Boise River flow at the Glenwood Bridge, which causes no flood damage downstream of Lucky Peak Dam, is 7,000 cfs (cubic per seconds). Flows greater than 7,000 cfs are considered as unregulated flows (Schmidt et al., 2013). The flood damage cost is estimated as a function of discharge at the Glenwood Bridge gaging station within the 500-year flood plain of the Boise River. The unregulated flows between 7,000 and 35,000 csf caused flood damage worth in the range of \$390K to \$329M, which is calculated based on the population and the price level in 1994. Schmidt et al. (2013) applied a multiplier of 2.5 to the flood damage estimate in order to consider inflation and population increase. Figure 0-3 shows the flood damage cost function that is derived based on the 2010 lower Basin population and prices (Schmidt et al., 2013).

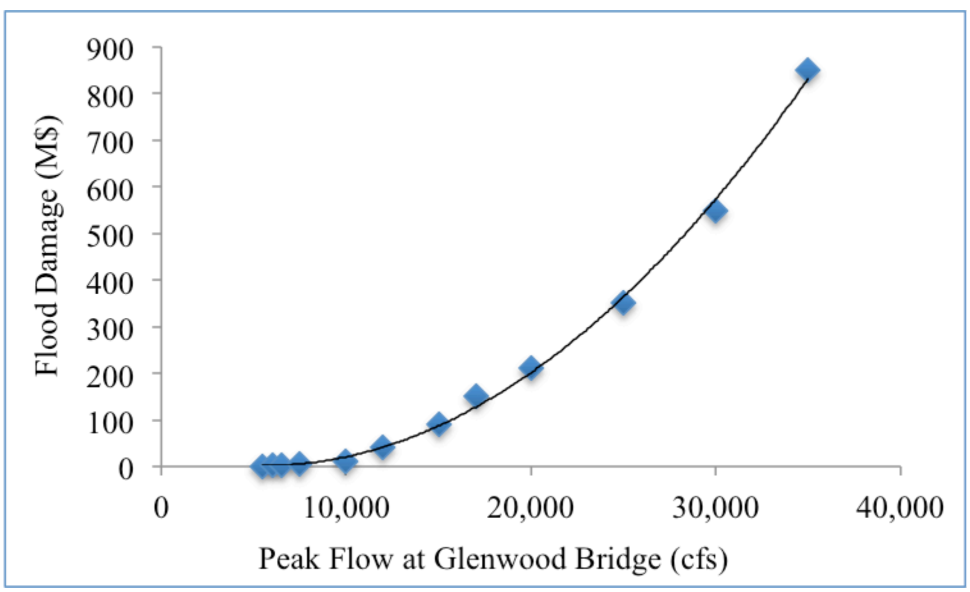

Figure 0-3 Flood Damage Function (Schmidt et al., 2013). The function is fitted as $\Phi = kq^2$, where k=1.01.

The flood damage parameter (k) is set to 1 in the empirical model. More accurate representation of the flood damages can be used in the next iteration of the model.

3.3 Objective Function: Water Release Benefit

The benefit of releasing water is determined by subtraction of flood damage cost from the agricultural water revenue, which has been multiplied by the irrigation demand seasonal shifter (Eq. 21). This is considered for the whole year from t=0 to t=365 days. The water year starts on October 1st and ends on September 30th. Hence,

$$\int_0^{365}[\psi(t)(\int_0^{q(t)} -0.0036\, q(t) + 220)\, dq(t)] - q(t)^2)\, dt \qquad (22)$$

3.4 Water Inflow

The required input data for daily inflow into Lucky Peak Dam is obtained from Bureau of Reclamation (BOR, 2014). Data for Lucky Peak Dam inflow is available as daily average values (cubic feet per second) from 1985 (earliest available data) to 2013. The "Water Years" are from October 1st to September 30th. Daily inflow into the reservoir (in acre feet unit) over time is presented in Figure 0-4. Fitting these daily inflow values as polynomial curves for 27 years using ordinary least squares (OLS) method, we obtain average daily inflow for a representative water year. *R* Squared (0.6) was used as the criteria for determining the best functional form.

$$\mu(t) = 1.0\times10^{-7}t^5 - 1.0\times10^{-4}t^4 + 0.0291t^3 - 2.9608\, t^2 + 98.847t + 232.43\ . \qquad (23)$$

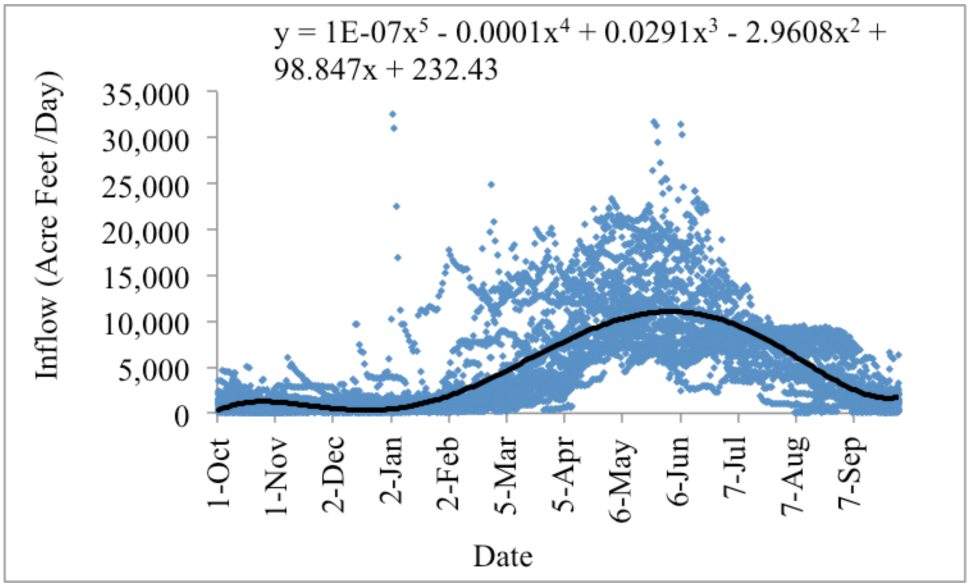

Figure 0-4 Daily inflow from 1985 to 2013. Data are fitted with a polynomial function.

Figure 0-5 shows irrigation water demand timing and average water inflow during a water year. It illustrates the time lag between peak irrigation water demand and peak water inflow.

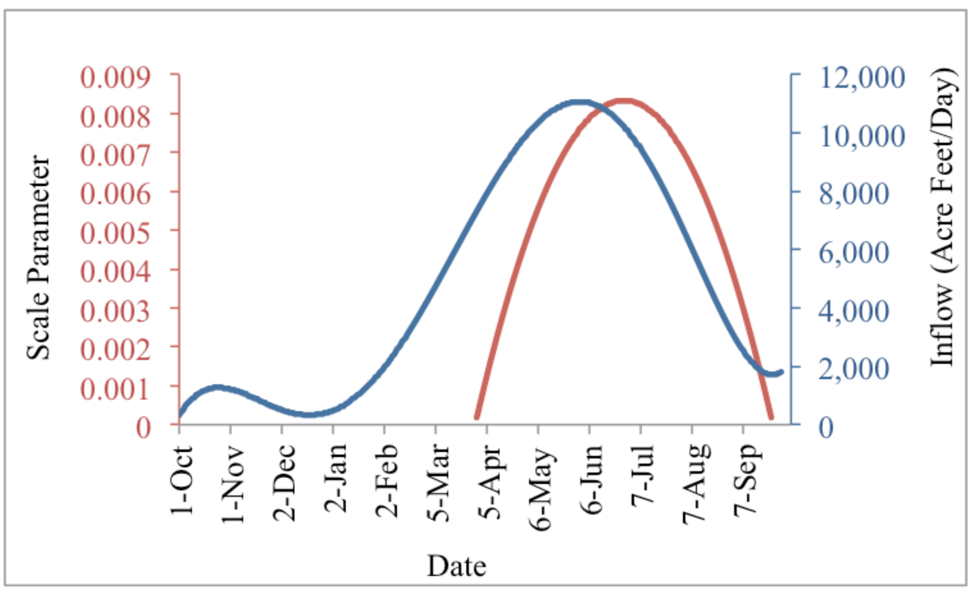

Figure 0-5 Water demand timing and inflow.

Chapter 4: Result and Discussion

The empirical model was solved using the non-linear programming optimization routine in GAMS (see appendix B) to derive the optimal water release during a water year. Figure 0-1 presents the water inflow (blue curve) and the optimized path of water release (red curve). The results show that the water inflow and the optimal water release start to rise in the beginning of the water year (October 1st) and show a small peak at late-October. From mid-November to the end of March, there is no release of water from the reservoir. The reason is that there is no agricultural water demand during this period and the water volume in the reservoir in that period is far below the maximum reservoir capacity is because of relatively low inflow (very low flood risk). From April until mid-May, inflow and release curves are identical and rising. In other words, the amount of released water is equal to the amount of inflow. From the beginning of June until the end of July, the two curves follow different paths as water release peaks to satisfy high irrigation demand. The optimal release increases to 17,000 (acre feet / day) in June. Beginning in August, the release and the inflow curves become identical again until the end of the water year.

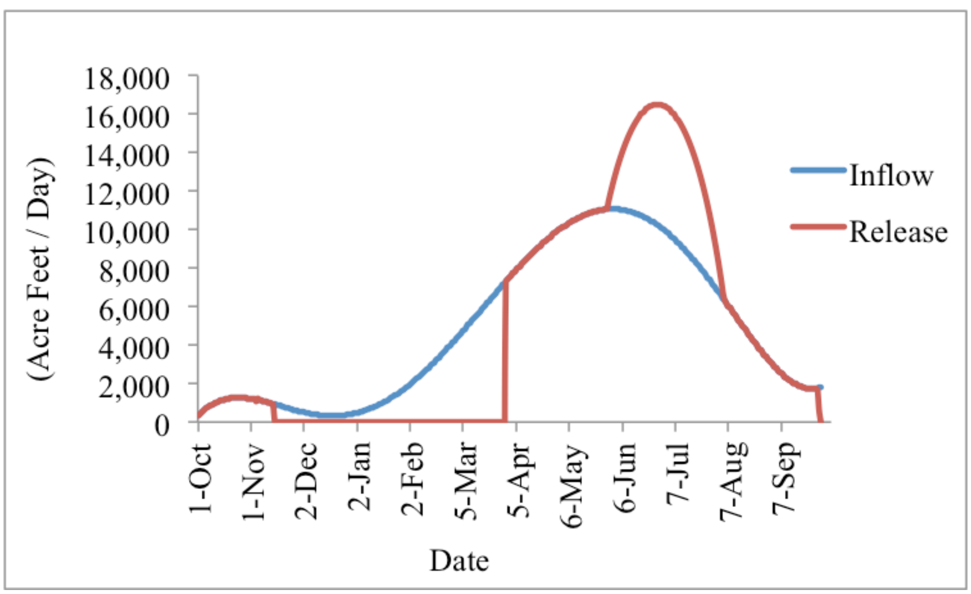

Figure 0-1 Water inflow and optimized water release path during one water year.

Figure 0-2 shows the reservoir water level during a water year, according to equation 3. From the middle of November to the end of March, water releases are zero and then gradually increase. Water accumulated during this period is used for irrigation during the high irrigation demand season (June, July). The reservoir water level in Figure 0-2 corresponds to the optimal water release path shown in Figure 0-1. The water level in the reservoir is constant when inflow and outflow are equal (April-May and August-October). The water level increases during the time when water release is zero (mid-November to the end of March), and decreases during the release peak time (mid-May to the end of July).

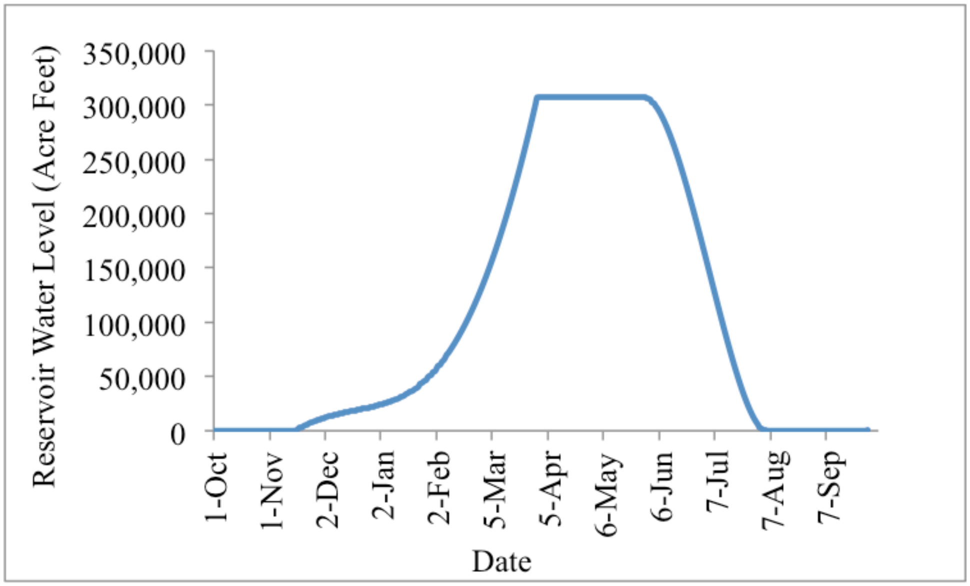

Figure 0-2 Reservoir water level during one water year.

The optimal water release results can be compared to the rule curves provided in Schmidt et al. (2013). Rule curves are used for the operation of a reservoir system (Ngo, 2006) in terms of water release timing and magnitude. Schmidt et al. (2013) used the Boise Basin reservoir system rule curves (Figure 4-3) to minimize flood damage given precipitation forecast. They illustrated the rule curves to show how flood control reservoirs are managed. For a given time and a corresponding forecast amount of cumulative inflow (runoff volume forecast from date through July 31st), the rule curves in Figure 0-3 indicate the minimum required space in the reservoir in order to accommodate future inflow and prevent potential floods. For example on April 1st, with 2 million acre feet of cumulative expected inflow; at least 600,000 acre feet space in the reservoir is needed.

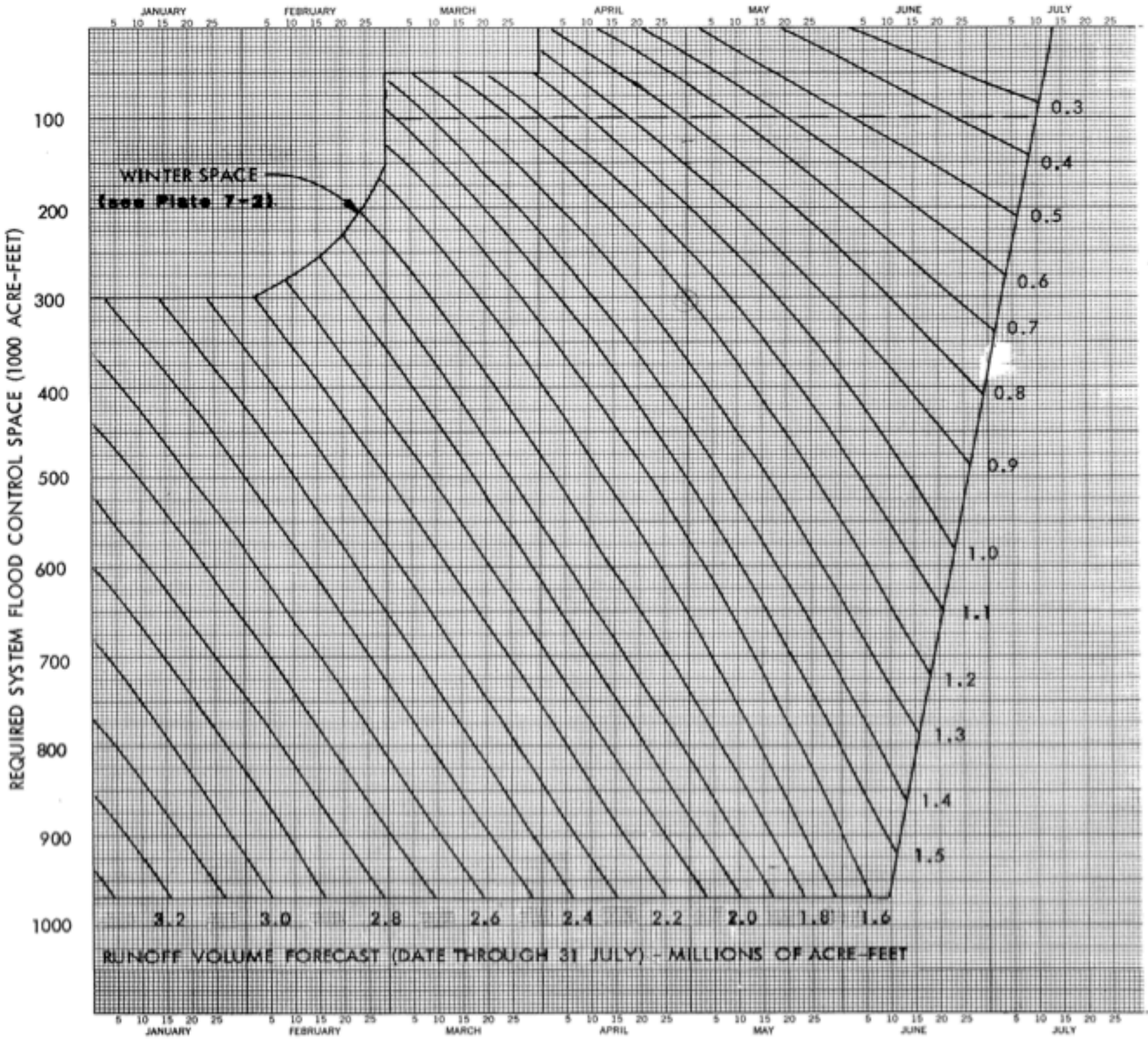

Figure 0-3 Boise Basin reservoir system flood control rule curves (Schmidt et al., 2013)

In order to compare our results with these rule curves, first runoff volume forecast (date through July 31st) are obtained (Figure 4-4). Runoff volume forecast values are measured as the area under the inflow curve (Figure 0-4) from each day through July 31st.

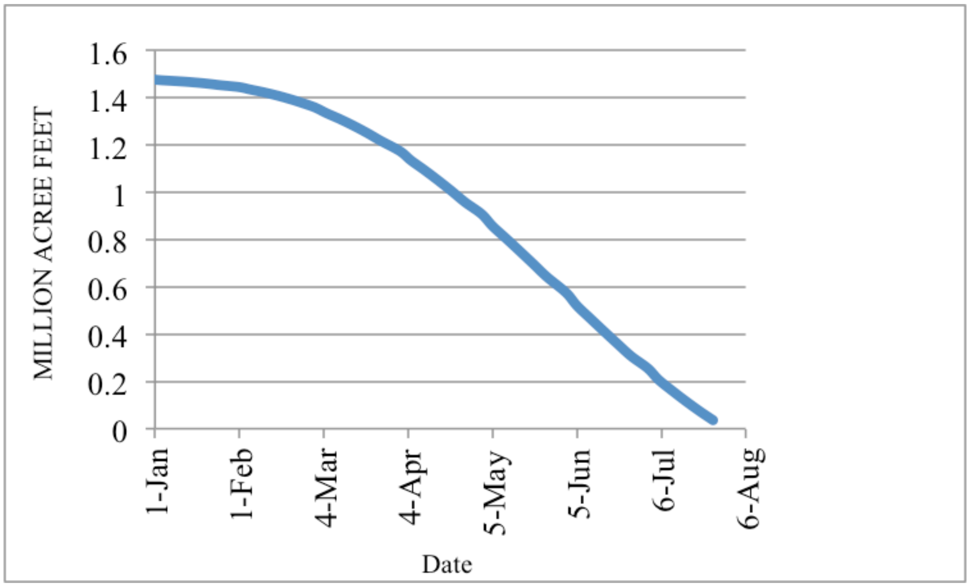

Figure 0-4 Runoff volume forecast (Date through July 31)

Then the required space for each cumulative forecast value over time using the rule curves in Figure 0-3 is tracked using cumulative inflow in figure 4.4. The obtained minimum required space over time is shown as the red line in Figure 0-5. The blue line in Figure 0-5 shows space availability in the reservoir according to solutions from the optimization model. These space values over time are obtained by subtracting the simulated reservoir water level (figure 4-2) from the reservoir capacity at each time during the year.

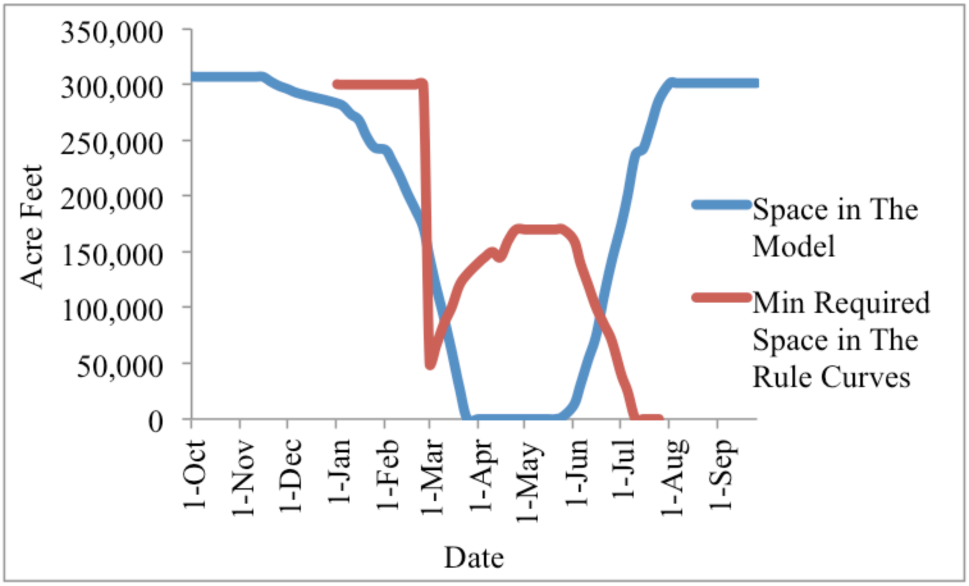

Figure 0-5 Reservoir space from the optimization model and minimum required space from the rule curves throughout a year.

Given the runoff forecast and the time of the year, the operating rule curves define the minimum required space to prevent flood throughout the year (the red curve in Figure 0-5). However, the optimization model seeks to find an optimum water release considering both agricultural water demand and flood control (the blue curve).

3.5 Climate Change Scenario

Idaho has seen significant temperature increases, especially in the past few decades. From 1971-2005, the average annual observed temperature in the Snake River Plain, located in southern Idaho, has increased by 1.4 degrees Celsius based on the data from 10 climate stations. Statistically, the increasing temperature trends are most significant in the months of January, March, and April (Hoekema and Sridhar, 2011).

Early runoff in response to warmer temperatures will have implications for agricultural production and water management. Winter precipitation is composed of more rain and less snow, which causes declining snowpack every year. Peak stream flows are occurring earlier in the year, which will consequently reduce summer flows. Peak spring runoff is occurring anywhere between a few days to 25-30 days earlier throughout the western US (Stewart, Cayan and Dettinger, 2004).

For the sake of sensitivity analysis, the effect of earlier runoff on optimal water release is examined. This study considers a 20-day shift in precipitation patterns. Figure 0-6 shows inflow data and the estimated expected inflow curve for the scenario with runoff occurring 20 days earlier compared to the regular inflow shown in Figure 0-4.

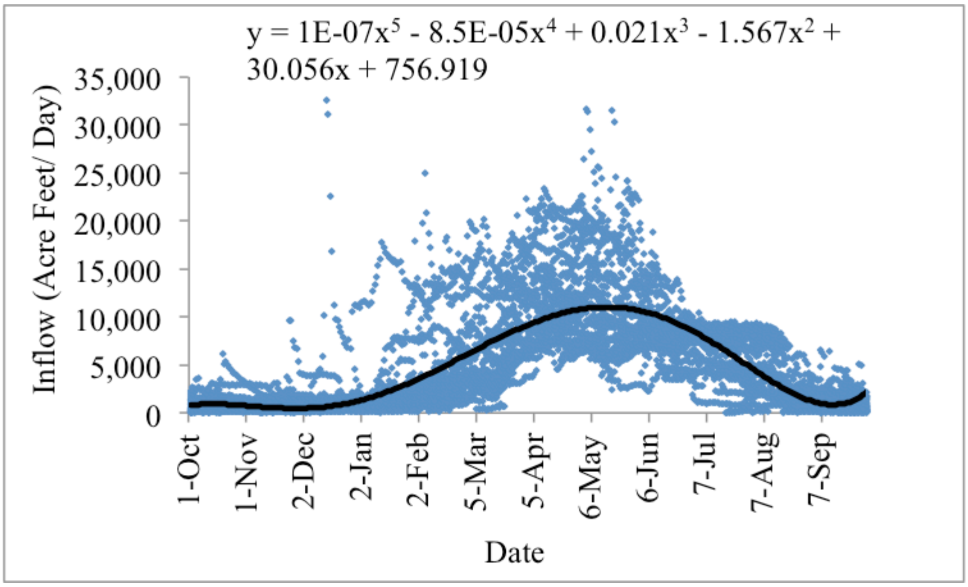

Figure 0-6 Lagged inflow curve (20 days).

The model is resolved with an updated inflow curve shown in Figure 0-6. The result is shown in Figure 0-7.

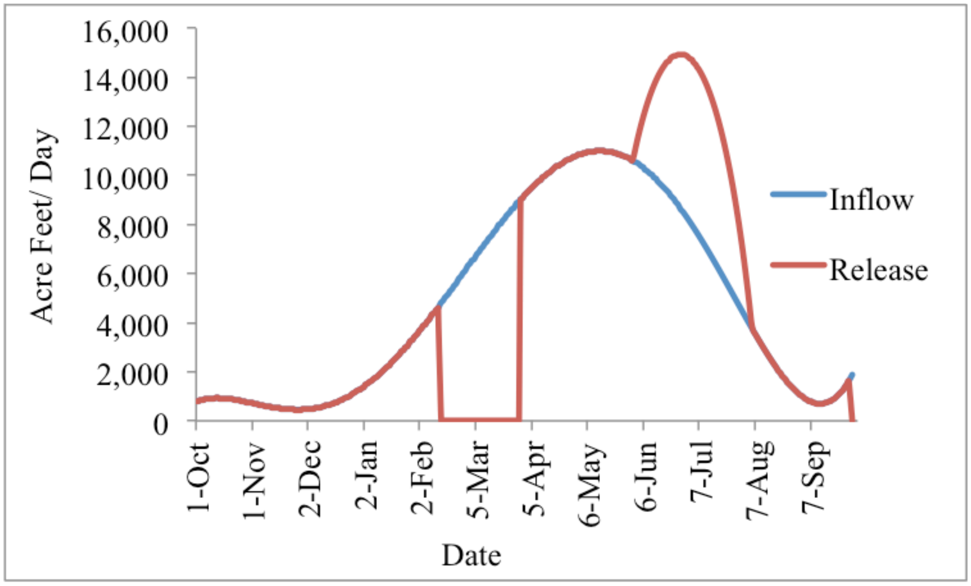

Figure 0-7 Derived water inflow and water release path for climate change scenario.

The optimal water release is altered as a result of earlier runoff. Specifically, early runoff reduces the water release peak in June from 17,000 acre feet in the regular model to 15,000 acre feet in the lagged model. We also have a shorter period where the least amount of water storage begins three months later in mid February.

Figure 0-8 shows how reservoir storage varies throughout the water year as a result of the earlier runoff. Compared to the baseline results in Figure 0-2, the reservoir water level starts to rise three months later (in February). However, the highest reservoir water level occurs almost at the same time (end of March) and the reservoir water level trajectory is qualitatively similar to baseline results.

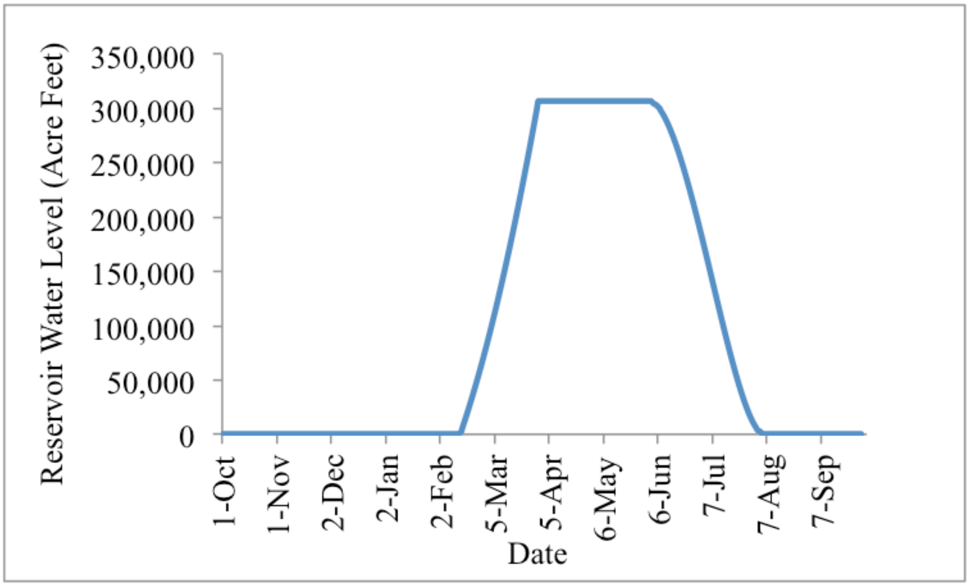

Figure 0-8 Reservoir water level for climate change scenario

Chapter 5: Conclusion

In this study an optimization model is used to examine the optimum amount of water release (q) throughout a representative water year for a multipurpose reservoir. Disregarding risk and uncertainty, the optimal solution prescribes a water release amount throughout the year, which satisfies irrigation water demand and leaves enough reservoir space for flood control. The analytic model derives and solves a differential equation, which balances the benefits from releasing water for irrigation and maintaining sufficient reservoir space for flood control during critical times of the year. For simplicity, the irrigation water demand is assumed to be a linear function and the flood damage cost is also illustrated as a simple quadratic function with respect to the water release. For more complicated functions, we would need to solve different differential equations with a higher order of complexity possibly using numerical methods. For example, exponential functions for irrigation water demand and/or flood damages could be investigated in future studies.

The water release solution in our model, as shown in Eq. 19, is a function of water inflow as well as coefficients in the linear water demand function and the quadratic flood damage cost. It can be seen in Eq. 20 that there is not a simple relation between q and other coefficients describing flood damage and water demand.

The empirical dynamic model is applied to Lucky Peak Dam as an illustration of the method. Following the analytical model, the irrigation water demand function is expressed in linear form. Flood damage is also expressed as an increasing linear function. The solution suggests releasing water in spring when the reservoir acquires the maximum amount of annual inflow. This result was expected because flood prevention is one of the primary purposes of Lucky Peak Dam's operation. From the middle of November to the end of March, water release decreases and the reservoir fills up to accumulate water for irrigation during summer months. These results are in contrast with the release implied by the rule curves. The reason for such a contrast is that the optimization model in this study is based on deterministic inflow. Stochasticity of inflow throughout the season is not taken into account. In practice, the decisions for reservoir operations are made in a stochastic environment where actual inflow during a water year deviates from predicted values. This thesis assumes perfect knowledge of future inflow. This knowledge allows the empirical model to operate on the edge, meaning that as long as future inflow is known, release can be equal to future inflow while keeping the reservoir full with no flood risk. The reason is that the inflow curve in this empirical analysis does not represent the extreme inflow values. Stochastic dynamic programming can be used to extend the model into stochastic context.

Climate changes in the form of an earlier runoff reduced the water release peak in June and resulted in a shorter empty reservoir season starting three months later in mid February. It implies that the agricultural benefits are affected adversely by early runoffs because of the water shortage (smaller peak) in high water demand months.

This study is not meant to provide either policy or scientific recommendations for reservoir management as far as flood control and irrigation water supply. Instead, the purpose of this work is to provide a preliminary analytical framework and spur further work. Numerous limitations in this study render the analysis inapplicable for practical purposes. However, the framework presented here can serve as a starting point for future modeling of joint reservoir management for flood control and irrigation water supply

It is important to keep in mind that the rule curves in Schmidt et al. (2013) are for the Boise reservoir system including Anderson Ranch, Arrowrock, and Lucky Peak Dam. The total space capacity for this system is 949,700 acre Feet, while the maximum capacity of Lucky Peak Dam, the only dam used in our empirical model, is 307,000 acre Feet (BOR, 2014). Furthermore, the inflow data also differs across the two reservoir systems.

It is also important to emphasize that the optimization model reflects runoff data for the past 27 years and uses a representative expected annual inflow. At this point the empirical optimization model does not consider runoff variability or uncertainty. Instead, the optimal water release schedule is obtained only for the expected future inflow. On the other hand, Figure 4-3 provides rule curves for a range of future runoff forecast values at any time of the year. Future extension of this work should consider stochasticity of runoff as a significant factor in balancing flood management and irrigation demand.

Although our model assumes a perfect knowledge of runoff, unexpected inflow is one phenomenon that is likely to be encountered during winter and spring. One major problem that leads to the unexpected inflow is climate change, which affects water resource management in a broad variety of ways. Global warming and corresponding changes in runoff can have a significant effect on water management.

Another limitation in this study is considering a low value crop water demand instead of the aggregate water demand. For illustrative purpose, the water demand function is limited to a low value crop water demand. Obviously, regarding aggregate water demand in the empirical model would yield to more accurate optimal water release result.

Finally, for simplicity, flood damage function was considered as a rough approximation of what it is in practice.

On the basis of this study, the following items can be pursued as natural extensions of this work:

1. Develop an empirical model for Boise Reservoir System to include other reservoirs in addition to Lucky Peak.
2. Develop a stochastic optimization model for daily operation by adding a stochastic component to the inflow.
3. Expand the intra-seasonal analysis model developed in this study to be inter-seasonal. In such a case, planted crop acreage will be a choice variable.
4. Calculate aggregate water demand as the horizontal summation of water demand-price for high value and low value crops, apply the aggregate water demand in the objective function of an empirical model and derive an optimal water release, which accounts for water demand for both low and high value crops.

References

Ahmad, S., Simonovic, S.P. (2000). System Dynamics Modeling of Reservoir Operations for Flood Management, *Journal of Computing in Civil Engineering*, 14(3): 190-198.

Bureau of Reclamation (BOR) (2014). Hydromet Historical Data Access, http://www.usbr.gov/pn/hydromet/arcread.html

Chang, J., Chen, L., Chang, L. (2005). Optimizing The Reservoir Operating Rule Curves By Genetic Algorithm, *Hydrological Process*, 19(11): 2277-2289.

Chatterjee, B., Howitt, R. E., Sexton, R. J. (1998). The Optimal Joint Provision of Water for Irrigation and Hydropower, *Journal of Environmental Economics and Management*, 36 (EE981047): 295-313.

Chen, L., McPhee, J., Yeh, W.–G. (2007). A Diversified Multiobjective GA for Optimizing Reservoir Rule Curves, *Advances in Water Resources*, 30(5): 1082-1093.

Contor, B.A., Taylor, G., Moore, G. (2010). Irrigation Demand Calculator: Spreadsheet Tool for Estimating Demand for Irrigation Water, WRRI Technical Report 200803, http://www.iwrri.uidaho.edu/documents/200803-1 revision.pdf ?pid =108520&doc=1

Das, T., Dettinger, M.D., Cayan, D.R., Hidalgo, H. G. (2011). Potential Increase in Floods in California's Sierra Nevada Under Future Climate Projections, *Climate Change,* 109 (suppl 1): S71-S94.

Federal Emergency Management Agency (FEMA) (2014). Benefits of Dams, http://www.fema.gov/benefits-dams.

Haddad, S., (2010). Capacity Choice and Water Management in Hydroelectricity Systems, *Energy Economics*, 33: 168-177.

Hoekema, S. (2011). Relating Climatic Attributes and Water Resources Allocation: A Study Using Surface Water Supply and Soil Moisture Indices in the Snake River Basin, Idaho. *Water Resources Research*, vol. 47 WO7536, doi: 10.1029/2010/WR009697.

Milly, P.C.D., Betencourt, J. M., Falkenmark, R.M., Hirsch, Z.W. Kudzewicz, D.P. Lettenmaier, Stouffer, R.J. (2008). Climate Change: Stationarity is Dead: Whither Water Management?" *Science*, 319: 573-574.

Nelson, C. G., Rosegrant. W.M., Koo, J., Roberstson, R., Susler, T., Zhu, T., Ringler. C., Msangi, S., Palazzo, A., Batka. M., (2009). Climate Change Impact on Agriculture and Costs of Adaptation. International Food Policy Research Institute.

Ngo, L.L. (2006). Optimizing Reservoir Operation a Case Study of the Hoa Binh Reservoir, Vietnam. Ph.D dissertation. Institute of Environment & Resources. Technical University of Denmark.

Palma. R.P., Xepapadeas A. (2004). Robust Control in Water Management, *The Journal of Risk and Uncertainty*, 29(1): 21-34.

Raff, D. A., Pruitt, T., Brekke, L.D. (2009). A Framework for Assessing Flood Frequency Based on Climate Projection Information, *Hydrology and Earth System Science*, 13: 2119-2136.

Raje, D., Mujumdar. P.P. (2010). Reservoir Performance Under Uncertainty in Hydrologic Impacts of Climate Change, *Advances in Water Resources*, 33: 312.

Roumasset, J., Wada, C.A. (2011). A Dynamic Approach to PES Pricing and Finance for Interlinked Ecosystem Services: Watershed Conservation and Groundwater Management, *Ecological Economics*, 87: 24.

Schmidt, R., Stodick, L., Taylor, G., Contor, B. (2013). Hydro-Economic Modeling of Boise Basin Water Management Responses to Climate Change, *Idaho Water Resource Research Institute Completion Report* 201301.

Stewart, I.T., Cayan, D.R., Dettinger, M.D. (2004). Changes in Snowmelt Runoff Timing in Western North America Under A "Business As Usual" Climate Change Scenario. *Climatic Change*, 62(1-3): 17-232.

Trezos, T., Yeh, W. (1987). Use of Stochastic Dynamic Programming for Reservoir Management, *Water Resources Research*, 23(6): 983-996.

Tung, C., Hsu, S., Liu, C., Li, J. (2003). Application of the Genetic Algorithm for Optimizing Operation Rules of the LiYuTan Reservoir in Taiwan, *Journal of the American Water Resources Association (JAWRA)*, 39(3): 649-657.

Trenberth, K.E. (2011). Changes in Precipitation with Climate Change, *Climate Research,* 47: 123.

USACOE (1995). Lower Boise River and Tributaries Reconnaissance Study, Walla Walla District, http://www.nww.usace.army.mil/Missions/Projects/LowerBoiseRiverFeasibilityStudy.aspx.

Appendix A

We derive a solution $j(t,s)$ for Eq.6 which satisfies the partial differential equation,

$$j(t,s) = \left(\frac{1}{2}\right)\left(2bs - 2a\mu s - 4k\mu s + \frac{1}{12(a+2k)(\theta_1-\theta_2)}((2b-2(a+2k)\mu)^2 - 4(b^2 - C_1 + 4ck - 4k\theta_1 s + 4k\theta_2 s + 4k\theta_1 s_{max} + 2a(c - \theta_1 s + \theta_2 s + \theta_1 s_{max})))^{3/2}\right) - \frac{C1t}{2(a+2K)} + C2 .$$

To prove this solution, we consider the PDE (Eq.6) and its derivatives with respect to t and s,

$$j_s = \frac{1}{2}\,(2b - 2a\mu - 4k\mu + \left((2b-2(a+2k)\mu)^2 - 4(b^2 - C1 + 4ck - 4k\theta_1 s + 4k\theta_2 s + 4k\theta_1 s_{max} + 2a(c - \theta_1 s + \theta_2 s + \theta_2 s + \theta_1 s_{max}))\right)^{1/2})$$

,

and

$$j_t = -\frac{C1}{2a+4k} \ .$$

Our PDE is

$$-j_t = \frac{-a}{2}\left(\frac{-J_s+b}{a+2k}\right)^2 + b\left(\frac{-J_s+b}{a+2k}\right) + c - k\left(\frac{-J_s+b}{a+2k}\right)^2 + J_s\left(\mu - \left(\frac{-J_s+b}{a+2k}\right)\right) + \theta_1 s\,(s_{Max} - s) + \theta_2\, s \ .$$

The right hand side of the PDE is

$$-(\frac{a}{2} + \mathrm{k})\,(\frac{-Js+b}{a+2k})^2 + b\left(\frac{-Js+b}{a+2k}\right) + c + Js\,\left(\mu - \left(\frac{-Js+b}{a+2k}\right)\right) + \theta_1(s_{max} - s) + \theta_2 s,$$

$= \quad c+\theta_2 s+\theta_1(s_{max}-s)+\frac{1}{a+2k}b[b+\frac{1}{2}(-2b+2a\mu+4k\mu-\{(2b-2(a+2k)\mu)^2-4(b^2-C1+4ck-4k\theta_1 s+4k\theta_2 s+4k\theta_1 s_{max}+2a(c-\theta_1 s+\theta_2 s+\theta_1 s_{max}))\}^{1/2})]+\frac{1}{(a+2k)^2}\left(-\frac{a}{2}-k\right)[b+\frac{1}{2}(-2b+2a\mu+4k\mu-\{(2b-2(a+2k)\mu)^2-4\left(b^2-C1+4ck-4k\theta_1 s+4k\theta_2 s+4k\theta_1 s_{max}+2a(c-\theta_1 s+\theta_2 s+\theta_1 s_{max})\right)\}^{\frac{1}{2}})]^2+\frac{1}{2}(2b-2a\mu-4k\mu+\{(2b-2(a+2k)\mu)^2-4(b^2-C1+4ck-4k\theta_1 s+4k\theta_2 s+4k\theta_1 s_{max}+2a(c-\theta_1 s+\theta_2 s+\theta_1 s_{max}))\}^{1/2})(\mu-\frac{1}{a+2k}\left[b+\frac{1}{2}(-2b+2a\mu+4k\mu-\{(2b-2(a+2k)\mu)^2-4\left(b^2-C1+4ck-4k\theta_1 s+4k\theta_2 s+4k\theta_1 s_{max}+2a(c-\theta_1 s+\theta_2 s+\theta_1 s_{max})\right)\}^{\frac{1}{2}})\right]).$

Now we consider *A* as

$(2b-2(a+2k)\mu)^2-4\left(b^2-C1+4ck-4k\theta_1 s+4k\theta_2 s+4k\theta_1 s_{max}+2a(c-\theta_1 s+\theta_2 s+\theta_1 s_{max})\right).$

The right hand side of the PDE is then written as

$c+\theta_2 s+\theta_1(s_{max}-s)+$

$$\frac{1}{a+2k}b\left[b+\frac{1}{2}\left(-2b+2a\mu+4k\mu-A^{\frac{1}{2}}\right)\right]+$$

$$\frac{1}{(a+2k)^2}\left(-\frac{a}{2}-k\right)[b+\frac{1}{2}(-2b+2a\mu+4k\mu-\ A^{\frac{1}{2}})]^2+$$

$\frac{1}{2}\left(2b-2a\mu-4k\mu+A^{\frac{1}{2}}\right)(\mu-\frac{1}{a+2k}\left[b+\frac{1}{2}\left(-2b+2a\mu+4k\mu-A^{\frac{1}{2}}\right)\right])$.

Simplifying each line, we have

$$c + \theta_2 s + \theta_1(s_{max} - s) +$$

$$\frac{b(-\sqrt{A} + 2\,(a+2k)\,\mu)}{2(a+2k)} +$$

$$-\frac{\left(\sqrt{A} - 2(a+2k)\mu\right)^2}{8(a+2k)} +$$

$$\frac{\sqrt{A}(\sqrt{A} + 2(b - (a+2k)\mu))}{4(a+2k)}$$

which is equal to

$$c + \theta_2 s + \theta_1(s_{max} - s) + \frac{b(-\sqrt{A}+2\,(a+2k)\,\mu)}{2(a+2k)} - \frac{\left(\sqrt{A}-2(a+2k)\mu\right)^2}{8(a+2k)} + \frac{\sqrt{A}(\sqrt{A}+2(b-(a+2k)\mu))}{4(a+2k)} =$$

$$c + \theta_2 s + \theta_1(s_{max} - s) + \frac{A-4(a+2k)\mu\,(-2b+(a+2k)\mu)}{8(a+2k)} =$$

$$c + \frac{A}{8(a+2k)} + b\mu - \frac{1}{2}(a+2k)\mu^2 - \theta_1 s + \theta_2 s + \theta_1 s_{max}\ .$$

Substituting A, we have

$$c + b\mu - \frac{1}{2}(a+2k)\mu^2 - \theta_1 s + \theta_2 s + \theta_1 s_{max} + \frac{1}{8(a+2k)}\Big((2b - 2(a+2k)\mu)^2 - 4\big(b^2 -$$
$$C1 + 4ck - 4k\theta_1 s + 4k\theta_2 s + 4k\theta_1 s_{max} + 2a(c - \theta_1 s + \theta_2 s + \theta_1 s_{max})\big)\Big) = \frac{C1}{2a+4k}\,,$$

which is equal to the left hand side of the PDE, $-j_t$. So the solution $j(t,s)$ is proven.

Appendix B

The non-linear programming model involved 4 equations used for both regular and climate change scenarios, and included the following assumptions and definitions.

Equations

1. *agricultural demands*
2. *reservoir water level*
3. *reservoir capacity*
4. *benefits*

The interpretation of the above equations is as follow:

Equation 1: Agricultural demand is considered as a linear function of t and water release in *t*. *b*(*t*) is the intercept and changes in respect to time and indicates how the water demand changes during the seasons (see water demand discussion in section 0).

Equation 2: Reservoir water level in every day (*t*) is the reservoir water level and the inflow in previous day (*t*-1) minus water release and flood in *t*-1. The order of *t* (days) is considered greater than 1.

Equation 3: The reservoir capacity is always a fixed value equal to 307,000.

Equation 4: The net benefit of water release is derived by the subtraction of flood damage in *t* from the ag demand value which is the area under agriculture water demand function from day 1 (Oct. 1^{st}) to day 360 (Sept. 30^{th}).

Appendix C

The function (ψ) for seasonality of irrigation water demand is expressed as follows:

ts is start date of irrigation. Assuming water year calendar starting from Oct 1, beginning of irrigation season is assumed at day 180

tm is peak irrigation, when irrigation reaches its peak in days starting from Oct 1st = 270.

*t*1 is the last day of irrigation = 360.

Variables:

$a1$ is the quadratic parameter.

$a2$ is the linear parameter.

$a3$ is the intercept.

Equations:

Equation1 = $a2 = -2a1tm$.

Equation 2 = $a1ts\ (ts + a2) + a3 = 0$.

Equation 3 = $\frac{a1t1^3}{3} + \frac{a2t1^2}{2} + a3t1 - \frac{a1ts^3}{3} - \frac{a2ts^2}{2} - a3ts = 1.$

The GAMS programming required for deriving the equation (ψ) in Figure 0-2 has been written based on the following principles; the water demand timing is assumed to follow a quadratic shape with roots 180 and 360, which indicate the starting date and ending date of water demand timing, respectively. In addition, the derivative of the equation is zero in day 270, which is assumed to have the peak demand for irrigation water. The area under the quadratic equation curve is assumed to be equal to one, which implies that this representation distributes the original value of the intercept, obtained from irrigation water demand functions in Schmidt et.al. (2013), across the irrigation season. The scale parameter for the equation (ψ) in Figure 0-2 is obtained by solving the system of three equations for the three unknown parameters.